Heliyon 9 (2023) e20184

Contents lists available at ScienceDirect

Heliyon

journal homepage: www.cell.com/heliyon

SERPINB7 as a prognostic biomarker in cervical cancer: Association with immune infiltration and facilitation of the malignant phenotype

Hua-Fang Wei [a], Rui-Feng Zhang [a,b], Yue-Chen Zhao [b], Xian-Shuang Tong [a,*]

[a] Department of Internal Medicine-1, Jilin Cancer Hospital, Changchun, Jilin, People's Republic of China
[b] Department of Radiation Oncology, The Second Hospital of Jilin University, Changchun, Jilin, People's Republic of China

ARTICLE INFO

Keywords:
Serpin family-B member 7
Cervical neoplasms
Prognosis
Tumor microenvironment
DNA methylation

ABSTRACT

Purpose: The purpose of this study was to investigate the expression patterns, predictive significance, and roles in the immune microenvironment of Serpin Family-B Member 7 (SERPINB7) in cervical squamous cell carcinoma and endocervical adenocarcinoma (CESC).
Methods: The expression of SERPINB7 and its prognostic relevance were evaluated using RNA-seq data from The Cancer Genome Atlas. SERPINB7 regulation of CESC cell growth and metastasis was investigated using MTT, scratch, and Transwell assays. *In vivo* effects of SERPINB7 were examined in xenograft model mice and differentially expressed genes (DEGs) associated with SERPINB7 were identified to explore its functional role in oncogenesis. Associations between SERPINB7 levels, chemosensitivity, and immune infiltration were assessed, and mutations and methylation of SERPINB7 were evaluated using the cBioPortal and MethSurv databases, respectively.
Results: SERPINB7 was up-regulated in CESC samples as well as in other tumors, and patients with higher SERPINB7A mRNA levels exhibited shorter overall survival. The area under the curve for the use of SERPINB7 in CESC diagnosis was above 0.9, and the gene was shown to regulate tumor cell proliferation and metastasis *in vitro* and *in vivo*. Overall, 398 DEGs enriched in key CESC progression-related signaling pathways were identified. SERPINB7 expression was additionally correlated with intratumoral immune infiltration and immune checkpoint activity. Patients expressing higher SERPINB7 levels exhibited distinct chemosensitivity profiles, and methylation of the SERPINB7 gene was linked to CESC patient prognostic outcomes.
Conclusion: SERPINB7 was found to be a crucial regulator of CESC progression, prognosis, and the tumor immune microenvironment, highlighting its potential as a diagnostic and prognostic biomarker and target for CESC immunotherapy.

1. Introduction

Cervical cancers (CCs) such as squamous cell carcinoma and endocervical adenocarcinoma (CESC) are ranked fourth worldwide in terms of cancer-associated deaths in women, with 604,127 new diagnoses and 341,831 deaths reported in 2020 [1]. Following the

* Corresponding author. Department of Internal Medicine-1, Jilin Cancer Hospital, NO.1066 Jinhu Road, Changchun, 130103, People's Republic of China.
E-mail address: TXS18843105707@163.com (X.-S. Tong).

https://doi.org/10.1016/j.heliyon.2023.e20184
Received 21 May 2023; Received in revised form 6 September 2023; Accepted 13 September 2023
Available online 15 September 2023

advent of CC assessments, including the Pap smear, thin prep cytological, and human papillomavirus tests, the incidence of CC has been reduced to a certain extent [2]. However, these screening approaches have shortcomings such as poor specificity and sensitivity, high requirements for laboratory conditions, and clinicians' operating skills. Moreover, patients with advanced CC in some economically underdeveloped areas have poor five-year disease-free survival (DFS) rates of <50% [3]. Hence, there is an urgent need for novel molecular markers and sophisticated approaches for deciphering the underlying molecular mechanisms of this cancer.

Bioinformatics technology is assuming an ever more vital role in tumor research, achieving noteworthy advancements in the discernment of prognostic markers and immunotherapy targets. Through the application of diverse bioinformatics techniques encompassing genomics, transcriptomics, and proteomics, a more profound comprehension of cancer's molecular mechanisms can be attained [4–6]. By scrutinizing extensive datasets such as TCGA, it can reliably forecast prognostic elements such as survival rates and disease progression in CESC. Moreover, the precise identification of immune antigens expressed on the surfaces of tumor cells can contribute substantially to the identification of immunotherapy targets, establishing a sturdy theoretical framework for personalized immunotherapeutic approaches.

Protein and polypeptide protease inhibitors are widely expressed in different organisms where they participate in many essential life activities. The serine protease inhibitor (Serpin) superfamily includes a wide variety of proteins with a broad distribution and diverse functions [7]. It has been found that most serpins, as regulatory factors, participate in fibrinolysis, coagulation, embryonic development, and the complement cascade *in vivo* [8,9]. The serpin superfamily is divided into A to P subtypes according to their sequence similarity, of which subtype B is the largest subfamily and consists mainly consists of intracellular serpins.

Serpin Family-B Member 7 (SERPINB7), also known as megsin, is expressed mostly in renal mesangial cells, and its expression is significantly increased in renal tissues of IgA and diabetic nephropathies. Deletion mutations or anomalous transcription of the SERPINB7 gene triggers the occurrence of Nagashima-type palmoplantar keratosis or psoriasis [10,11]. It has also been found that SERPINB7 regulates cell proliferation, signal transduction, and extracellular matrix metabolism. Furthermore, data showed that SERPINB7 expression was linked with tumorigenesis in lung and breast tissues, where SERPINB7 is overexpressed, and its expression levels were linked to tumor cell metastasis and propagation [12]. Nevertheless, the exact role of SERPINB7 in CESC and its underlying mechanisms are as yet unclear.

To assess the role and predictive significance of SERPINB7, we investigated its transcription levels in CESC, using data retrieved from The Cancer Genome Atlas (TCGA). In addition, the molecular functions of SERPINB7 in the development of the disease were further studied *in vitro* and *in vivo*. We also correlated SERPINB7 transcription levels with immune cell infiltration of cervical tumor tissue, investigated changes in the expression of immune checkpoints, and evaluated chemosensitivity. These findings provide new evidence for further research on the role of SERPINB7 in CESC and provide a solid foundation for the development of accurate diagnostic procedures and treatment of CESC.

2. Materials and methods

2.1. Data collection

The SERPINB7 transcription profiles of samples from CESC patients together with data on patient clinical and other relevant medical information, including age, TNM stage, clinical and G stage, were obtained from the TCGA platform. The CESC patients were divided into high SERPINB7- and low SERPINB7-expression groups according to the median level of SERPINB7 mRNA expression.

2.2. Patients and clinical specimens

Eight pairs of CESC and matched adjacent normal cervical tissues were collected from patients treated at the Second Hospital of Jilin University from January 2022 to August 2022. The inclusion criteria were 1) primary CESC samples with a definite diagnosis and 2) without radiotherapy or chemotherapy before surgery. The Medical Ethics Committee approved the study (Second Hospital of Jilin University - NO.2022–107).

2.3. Immunohistochemical (IHC) analysis

Tissue sections were incubated with a rabbit anti-SERPINB7 polyclonal antibody (1: 200; Abcam, UK) overnight at 4 °C, followed by incubation with a goat anti-rabbit secondary antibody (1:200; Abcam; 120 min, room temperature [RT]). The color was developed using DAB (3,3′-diaminobenzidine) chromogenic solution (Absin, China). The nuclei were counterstained with hematoxylin (Beyotime, China) for 3 min at RT. The sections were desiccated, preserved with Histo-Clear, sealed with neutral balsam, and visualized under light microscopy (CTR600, Leica, Germany).

2.4. Western blot analysis

Proteins were extracted from the tissues after lysis with RIPA buffer (Solarbio, China) and were separated on 10% SDS-PAGE gels (Beyotime) using an electrophoresis system (Bio-Rad, USA) at 200 V for 40 min. The proteins were then transferred to PVDF membranes (Millipore, USA) using a protein transfer instrument (Bio-Rad; 400 mA/30 min). After blocking, the membranes were incubated with a rabbit anti-SERPINB7 polyclonal antibody (1:1000) or rabbit anti-histone H3 polyclonal antibody (1:1000; Abcam; 4 °C/overnight) followed by incubation with a secondary goat anti-rabbit antibody (1:10,000; 120 min/RT). Protein bands were visualized

using the BeyoECL Plus Kit (Beyotime).

2.5. Real-time quantitative PCR (RT-qPCR)

RNA samples were extracted from transfected cells using TRIzol reagent (Tiangen, China). Subsequently, cDNA was synthesized from the RNA using a First Strand cDNA Synthesis Kit (TaKaRa Bio, Japan). RT-qPCR was performed on an ABI PRISM 7000 Sequence Detection System (Applied Biosystems, USA). The primer sequences specific for SERPINB7 that were used were: forward: 5′-AAATGCAGAGTTTTGCTTCAACC-3′, reverse: 5′-GAAGAGTTTCCATATCCTGAGGC-3′. Relative expression of SERPINB7 was calculated using the $2^{-\Delta\Delta CT}$ method with GAPDH as the internal control.

2.6. Cell culture and short hairpin RNA (sh-RNA) interference protocol for SERPINB7 knockdown

The HeLa human adenocarcinoma cell line (CL-0101, Procell, China) was grown in MEM (Procell), supplemented with 10% fetal bovine serum (FBS) (Procell) under optimal conditions (37 °C, 5% CO_2). Individual lentiviral vectors (Genechem, China) containing SERPINB7 short-hairpin RNA (sh-SERPINB7) or negative control (sh-NC) were synthesized and then used to infect HeLa cells via the Lipofectamine 3000 kit (Invitrogen, USA) to establish stably transfected cell lines. After 12 h, the stably transfected cells were selected using puromycin following the manufacturer's instructions. Cells were collected 48 h after transfection and used for subsequent experiments. The transfection efficiency was evaluated through RT-qPCR analysis at 24 h post-transfection.

2.7. 3-(4, 5-Dimethylthiazol-2-yl)-2, 5-diphenyltetrazolium bromide (MTT) assay

The transfected HeLa cells (1×10^5 cells/mL) in each group were seeded in 96-well plates after 48 h of transfection. Ten microliters of MTT reagent (Procell) were added to each well, with five replicates for each condition. After incubation for 3 h at 37 °C, absorbances at 570 nm were read in a microplate reader (Bio-Rad, model 550).

2.8. Scratch assay

Transfected HeLa cells were plated in 6-well plates and grown until confluent. Longitudinal scratches were made in the cell monolayer using a 20 μL pipette tip. At 0 h or 24 h after scratching, the widths of the scratches were imaged under light microscopy and the cell migration was assessed by ImageJ software using the formula: cell migration index = (0 h scratch width - 24 h scratch width)/0 h scratch width.

2.9. Cell metastasis assay

Transfected HeLa cells in serum-free medium were seeded in a Matrigel®-pre-treated upper chamber of a Transwell system (BD Biosciences, USA). The lower chamber contained MEM with 10% FBS. The cells were cultured for 24 h, after which invading cells were fixed with 4% paraformaldehyde (Beyotime) and stained with Giemsa (Solarbio). The invasive cells from randomly selected fields were counted under light microscopy (100 ×) and statistically analyzed.

2.10. In vivo research

BALB/cA-nu mice (6–8 weeks; 18–20 g) were used in the *in vivo* experiments. Sh-SERPINB7- or sh–NC–transfected HeLa cells (1×10^7) were inoculated subcutaneously in the animals. Each of the sh-SERPINB7 and sh-NC groups consisted of three mice. Tumor growth was monitored and the lengths and widths of the tumors were measured with vernier calipers. The mice were euthanized by cervical dislocation after 21 days. The tumors were photographed and weighed and the volumes were calculated as tumor volume = (length × width^2)/2. The tumor tissues were fixed in 4% tissue fixative and stained with hematoxylin-eosin. The animal experiments were approved by The Animal Care and Use Committee of Jilin University and were performed following NIH guidelines.

2.11. Identification of differentially expressed genes and their functional implications in CESC

Genes expressed differentially between the samples were investigated and samples were divided into SERPINB7 high- and low-expression groups according to the median SERPINB7 expression level. The Limma package in R software was used to identify differentially expressed genes (DEGs) associated with SERPINB7 in the TCGA CESC data [13]. Data were quantified by the construction of volcano plots using FDR-optimized P-values <0.05/fold-change >1.5 as criteria. The top 50 upregulated and downregulated DEGs were displayed in a heatmap. Functional analyses were performed using Gene Ontology (GO) and Kyoto Encyclopedia of Genes and Genomes (KEGG) enrichments.

2.12. Association between SERPINB7 activity and the tumor microenvironment (TME)

Single-sample GSEA (GSVA package in R) was used for the assessment of immune infiltration [14,15]. The infiltration levels of twenty-four immune cell types were identified. The transcripts relevant to immune checkpoints were SIGLEC15, TIGIT, CTLA4,

CD274, HAVCR2, LAG3, PDCD1, and PDCD1LG2, and the expression data of these eight genes were extracted. The expression of immune checkpoints was compared between the SERPINB7 low- and high-expression groups using the Wilcoxon test.

2.13. Prediction of chemosensitivity

Reactions to chemotherapy were predicted in the CESC specimens using the publicly available Genomics of Drug Sensitivity in Cancer database (https://www.cancerrxgene.org/), using the "pRRophetic" package in R. The half-maximal inhibitory concentrations (IC_{50}) in the samples were assessed through ridge-regressional levels, with all variables pre-set at default levels [16]. The same grouping of CESC samples (high- and low-expression groups) based on the median expression level of SERPINB7 was used. The significance of the two groups of samples passed the Wilcoxon test.

2.14. Analysis of gene alterations and methylation

The TCGA (Firehose Legacy and PanCancer Atlas) databases allowed analysis of SERPINB7 expression procured through cBioPortal (www.cbioportal.org). Kaplan-Meier curves with log-rank tests were used for assessment of survival. DNA methylation data were retrieved from MethSurv (biit.cs.ut.ee/methsurv/). Furthermore, the predictive values of CpG methylation in SERPINB7 were studied. The survival outcome was calculated.

2.15. Statistical analyses

R (v. 3.3.1) was used for all analyses. Wilcoxon tests were used for comparisons between the two groups. pROC software was used for the construction of ROC curves for the evaluation of significance. Chi-square tests were used to evaluate associations between SERPINB7 levels and patient characteristics. Based on the median SERPINB7 mRNA expression level, 306 CESC patients were classified into high and low SERPINB7-expression groups. Kaplan-Meier curves were constructed to compare differences in the overall survival (OS) between groups, and P-values were calculated using the log-rank test in the survival package in R. The prognostic indicators for CESC were identified through univariate and multivariate Cox regression analyses. Cytotoxicity of tested chemotherapeutic medications was assessed through analyses of the IC_{50} values. P-values <0.05 values were considered statistically significant.

3. Results

3.1. SERPINB7 expression in various tumors

The flowchart of the entire research was shown in Fig. 1. SERPINB7 expression in various tumors was assessed using the pan-cancer TCGA database. Eleven tumors showed overexpression of SERPINB7, namely, BLCA, BRCA, CESC, COAD, ESCA, HNSC, LUAD, LUSC, READ, THCA, and UCEC. Conversely, SERPINB7 was downregulated in GBM, KICH, KIRC, and KIRP tumors (Fig. 2A). In CESC, SERPINB7 expression was found to be significantly higher in tumor samples compared with normal tissue ($P < 0.001$) (Fig. 2B). SERPINB7 expression was also correlated with the clinical characteristics of patients. Fig. 2C–I demonstrate that SERPINB7 expression

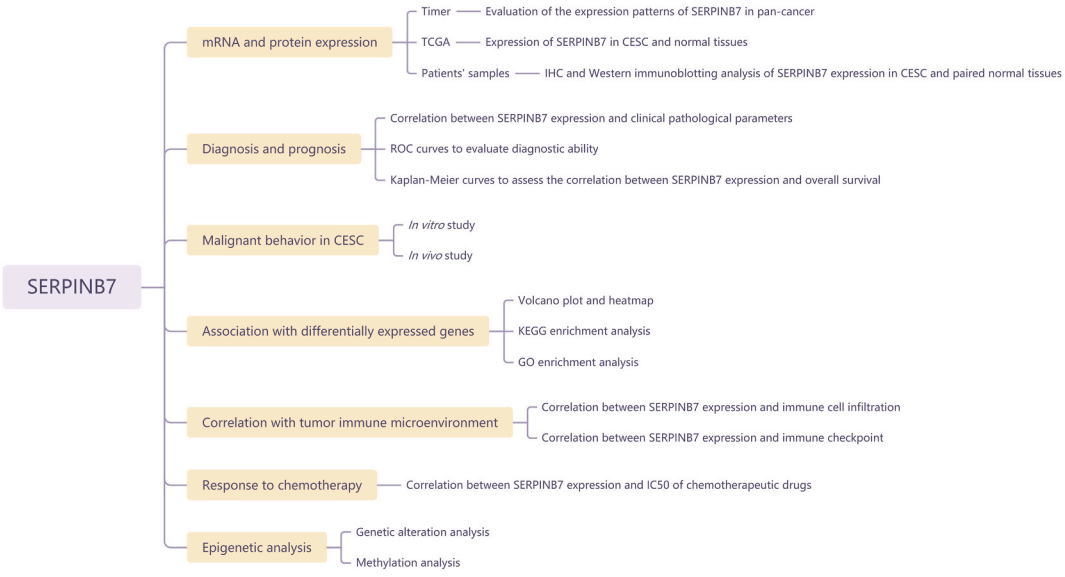

Fig. 1. The flowchart of the entire research.

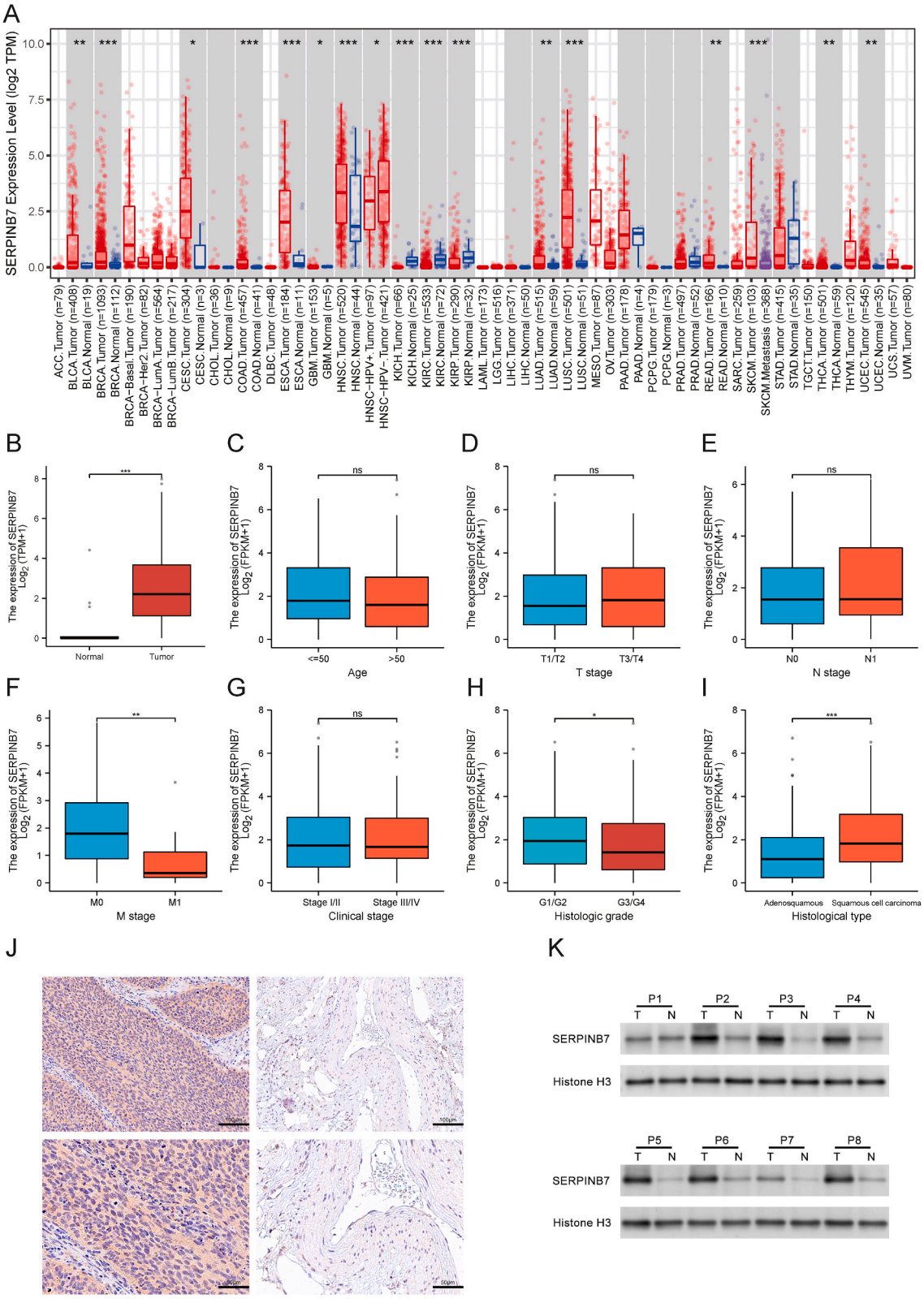

(caption on next page)

Fig. 2. Expression of SERPINB7 in pan-cancer and CESC based on analysis of TCGA data, IHC, and Western blotting. (A) SERPINB7 transcription levels in tumor and paired normal tissue samples from Timer pan-cancer data. (B) SERPINB7 expression levels in CESC tissues compared to normal tissues. This elevated expression was found to be significantly correlated with various clinicopathological characteristics, including (F) M stage, (H) histological grade, and (I) histological type. However, there was no significant association observed with (C) age, (D) T stage, (E) N stage, and (G) clinical stage. SERPINB7 expression was elevated in cancerous tissues of eight CESC patients compared with matched noncancerous tissues, shown by (J) IHC staining (× 200 and × 400) and (K) Western blotting. ns = not significant; *P < 0.05, **P < 0.01, ***P < 0.001. Abbreviations: ACC, Adrenocortical carcinoma; BLCA, Bladder Urothelial Carcinoma; BRCA, Breast invasive carcinoma; CESC, Cervical squamous cell carcinoma and endocervical adenocarcinoma; CHOL, Cholangiocarcinoma; COAD, Colon adenocarcinoma; DLBC, Lymphoid Neoplasm Diffuse Large B-cell Lymphoma; ESCA, Esophageal carcinoma; GBM, Glioblastoma multiforme; HNSC, Head and Neck squamous cell carcinoma; KICH, Kidney Chromophobe; KIRC, Kidney renal clear cell carcinoma; KIRP, Kidney renal papillary cell carcinoma; LAML, Acute Myeloid Leukemia; LGG, Brain Lower Grade Glioma; LIHC, Liver hepatocellular carcinoma; LUAD, Lung adenocarcinoma; LUSC, Lung squamous cell carcinoma; MESO, Mesothelioma; OV, Ovarian serous cystadenocarcinoma; PAAD, Pancreatic adenocarcinoma; PCPG, Pheochromocytoma and Paraganglioma; PRAD, Prostate adenocarcinoma; READ, Rectum adenocarcinoma; SARC, Sarcoma; SKCM, Skin Cutaneous Melanoma; STAD, Stomach adenocarcinoma; TGCT, Testicular Germ Cell Tumors; THCA, Thyroid carcinoma; THYM, Thymoma; UCEC, Uterine Corpus Endometrial Carcinoma; UCS, Uterine Carcinosarcoma; UVM, Uveal Melanoma.

was significantly associated with tumor M stage ($P < 0.01$), and histological grade and type ($P < 0.05$ and $P < 0.001$, respectively). However, no associations were seen with patient age, T, N, or clinical stage ($P > 0.05$). Furthermore, IHC staining and Western blotting showed that SERPINB7 was overexpressed in tumor samples compared with normal tissues (Fig. 2J–K). These data were similar to the results retrieved from the TCGA database.

3.2. SERPINB7 expression in CESC is strongly associated with clinical manifestations

The data from the TCGA was divided into the high and low SERPINB7-expression groups. The specific demographic and clinical data of the patients, such as age, TNM classification, G classification, and clinical classification, are shown in Table 1. The results showed associations between SERPINB7 transcription levels and patient weight ($P = 0.014$) and histological typing and grade ($P = 0.034$ and $P = 0.020$, respectively).

3.3. SERPINB7 has diagnostic and prognostic value in CESC

ROC curves were constructed using the SERPINB7 expression data (Fig. 3A). The area under the curve (AUC) value was 0.965, indicating outstanding diagnostic capacity. Comparison of AUC values for different CESC tumor stages showed strong consistency, with AUC values of 0.964 for stage I, 0.970 for stage II, 0.976 for stage III, and 0.919 for stage IV (Fig. 3B–E). SERPINB7 levels were thus sufficient to discriminate between early and late CESC stages (note the AUC of 0.507 for stages I/II against stages III/IV) (Fig. 3F).

Table 1
SERPINB7 expression is associated with clinical data from CESC individuals.

Characteristics	Variable	No. of patients	SERPINB7 mRNA expression		P value
			Low, n (%)	High, n (%)	
Age	≤50	188	90 (29.4%)	98 (32%)	0.411
	>50	118	63 (20.6%)	55 (18%)	
Weight	≤70	138	60 (21.7%)	78 (28.2%)	**0.014**
	>70	139	82 (29.6%)	57 (20.6%)	
T stage	T1	140	71 (29.2%)	69 (28.4%)	0.806
	T2	72	41 (16.9%)	31 (12.8%)	
	T3	21	10 (4.1%)	11 (4.5%)	
	T4	10	5 (2.1%)	5 (2.1%)	
N stage	N0	134	70 (35.9%)	64 (32.8%)	1.000
	N1	61	32 (16.4%)	29 (14.9%)	
M stage	M0	116	55 (43.3%)	61 (48%)	0.062
	M1	11	9 (7.1%)	2 (1.6%)	
Clinical stage	Stage I	162	82 (27.4%)	80 (26.8%)	0.809
	Stage II	69	33 (11%)	36 (12%)	
	Stage III	46	22 (7.4%)	24 (8%)	
	Stage IV	22	13 (4.3%)	9 (3%)	
Histological type	Adenosquamous	53	34 (11.1%)	19 (6.2%)	**0.034**
	Squamous cell carcinoma	253	119 (38.9%)	134 (43.8%)	
Histologic grade	G1	19	8 (2.9%)	11 (4%)	**0.020**
	G2	135	59 (21.5%)	76 (27.7%)	
	G3	119	72 (26.3%)	47 (17.2%)	
	G4	1	1 (0.4%)	0 (0%)	
Radiation therapy	No	122	58 (19%)	64 (20.9%)	0.559
	Yes	184	95 (31%)	89 (29.1%)	

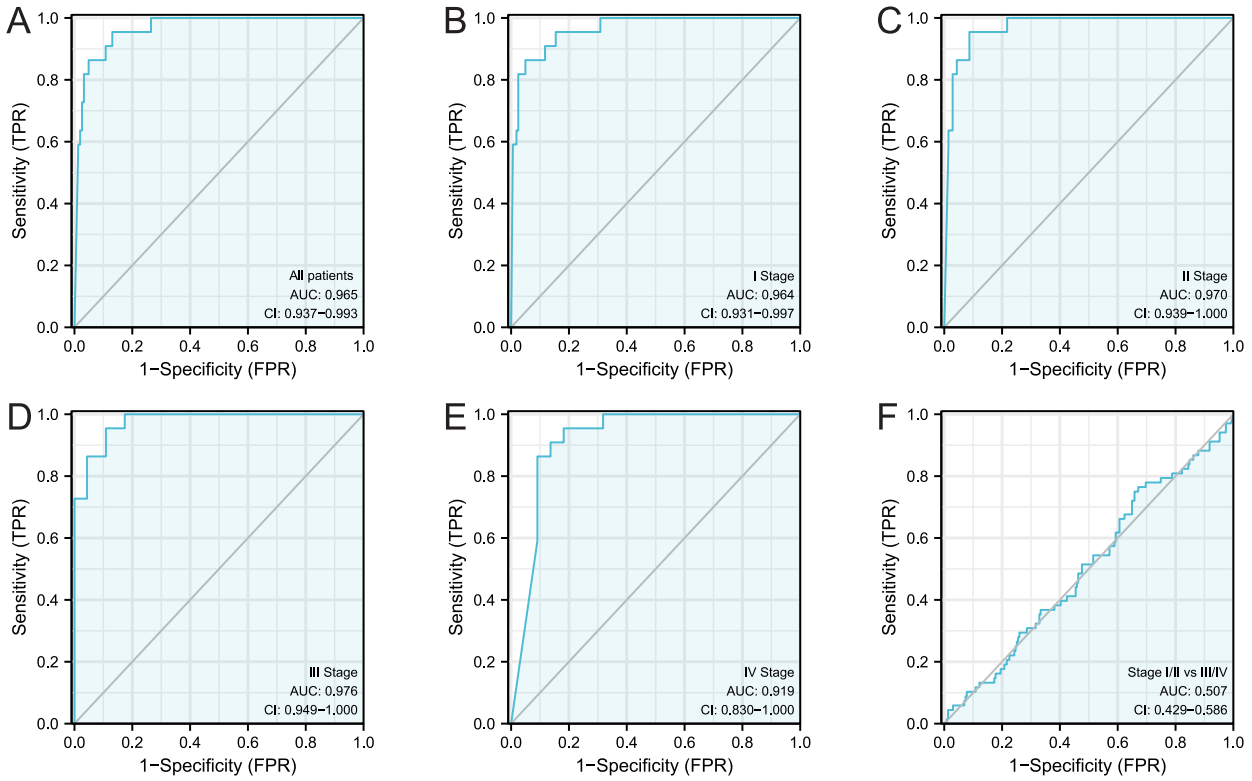

Fig. 3. ROC curves showing that SERPINB7 has outstanding diagnostic ability in CESC cohorts at all stages. (A) Healthy vs cancer samples. (B) Healthy vs stage I cancer samples. (C) Healthy vs stage II samples. (D) Healthy vs stage III tumor samples. (E) Healthy vs stage IV tumor samples. (F) Stage I/II against stage III/IV tumor samples.

3.4. Prognostic role of SERPINB7 in CESC

Kaplan-Meier curves further analyzed the ability of SERPINB7 expression levels to predict survival outcomes. These showed that SERPINB7 overexpression was linked to poor patient survival rates ($P = 0.01$) (Fig. 4A). Examination of CESC subgroups showed that SERPINB7 expression was correlated with survival rates in younger patients ($P = 0.002$) and with staging as follows: T1/T2 ($P = 0.004$), N0 ($P = 0.004$), N1 ($P = 0.008$), I/II ($P = 0.003$), and G1/G2 ($P = 0.03$). However, in older patients, SERPINB7 expression had no prognostic value ($P = 0.429$), with staging as follows: T3/T4 ($P = 0.267$), M0 ($P = 0.143$), M1 ($P = 0.292$), III/IV ($P = 0.783$), G3/G4 ($P = 0.216$) (Fig. 4B-M). Interestingly, patients with high SERPINB7 expression in N1 staging exhibited improved survival outcomes. This observation suggests the possibility of false-positive results, likely arising from the limited sample size within this subgroup. The univariate analysis revealed that poor OS was significantly associated with T stage ($P < 0.001$), N stage ($P = 0.002$), M stage ($P = 0.023$), clinical phase ($P < 0.001$) and SERPINB7 expression ($P = 0.013$). Multivariate analysis showed that T stage and SERPINB7 expression levels were independent risk factors for CESC outcomes (hazard-ratio = 19.827, $P = 0.001$; hazard-ratio = 1.674, $P = 0.009$) (Table 2).

3.5. In vitro and in vivo studies confirmed SERPINB7 participation in the development of CESC

SERPINB7 was silenced by sh-RNA in HeLa cells and the knockdown efficiency was verified by RT-qPCR (Fig. 5A). MTT assays showed that SERPINB7 knockdown inhibited HeLa cell proliferation compared to the control ($P < 0.05$) (Fig. 5B). Furthermore, SERPINB7 knockdown decreased tumor cell invasion and migration in the Transwell ($P < 0.001$) and scratch tests ($P < 0.001$) (Fig. 5C–D). Our *in vivo* analyses confirmed these results. The SERPINB7-silenced HeLa cells were inoculated in nude mice, and the characteristics of the tumors were studied after 21 days. The xenograft mouse model showed that the tumor weights in the sh–NC–transfected control and sh-SERPINB7-silenced groups were 147.33 ± 19.15 mg and 82.00 ± 26.09 mg, respectively ($P < 0.05$) (Fig. 6A–B) while the tumor volumes were 140.67 ± 10.04 mm^3 and 77.39 ± 19.30 mm^3, respectively ($P < 0.05$) (Fig. 6C). Furthermore, compared to the sh-NC group, the tumor tissues in the sh-SERPINB7 group showed that the nuclei were reduced in size with less intense staining. Typical cells are indicated by red arrows (Fig. 6D).

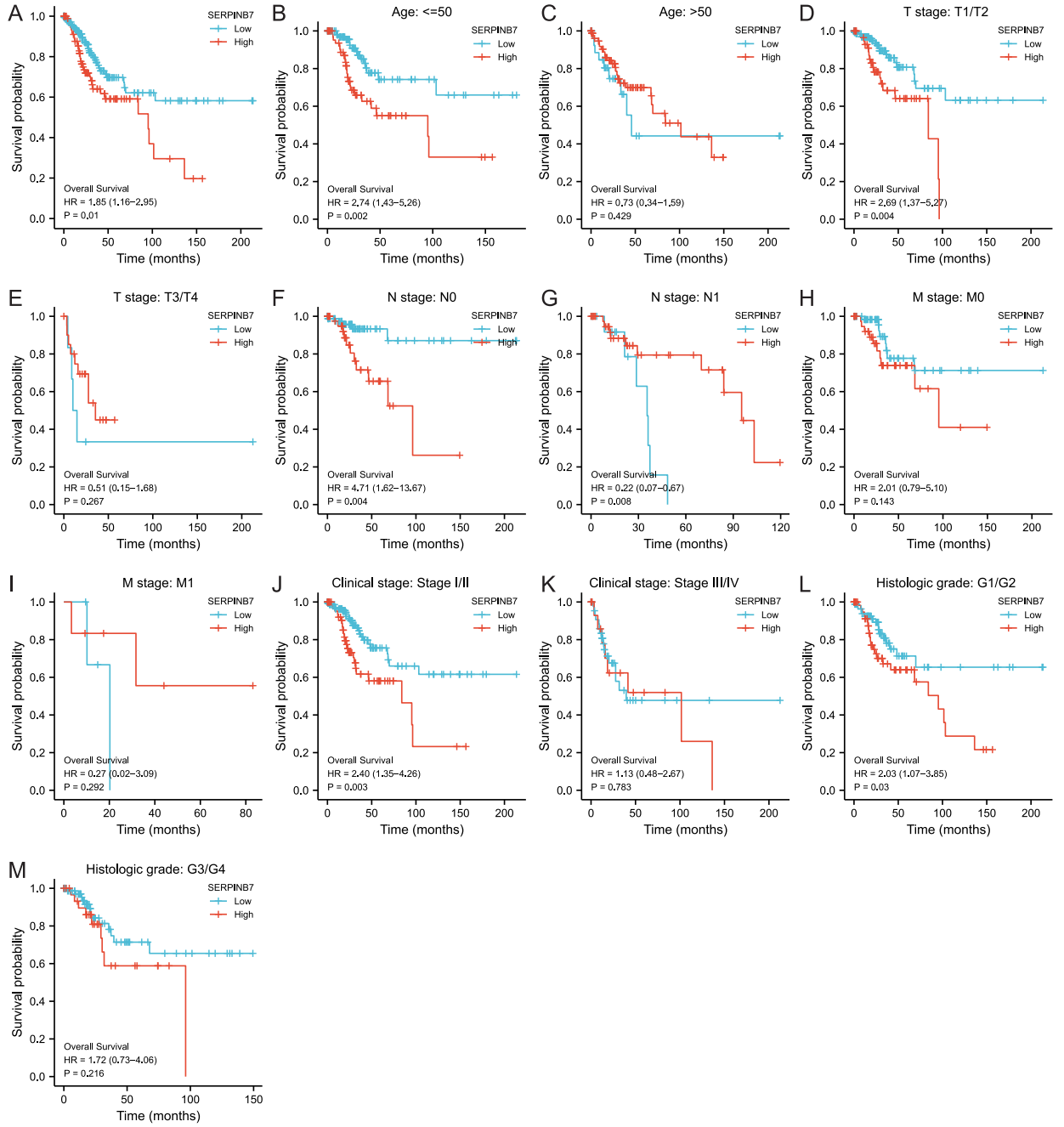

Fig. 4. Associations between SERPINB7 expression and OS outcomes. Patients were categorized into high- and low-expression cohorts based on the median expression level of SERPINB7. (A) Patients with elevated SERPINB7 expression had unfavorable OS. Elevated SERPINB7 expression was associated with unfavorable OS in patients with (B) age≤50, (D) T1/T2 stage, (F) N0 stage, (J) I/II clinical stage, and (L) G1/G2 grade. Conversely, patients with (G) N1 stage exhibited satisfactory OS with elevated SERPINB7 expression. However, no significant correlations were observed between SERPINB7 expression and OS in patients with (C) age≥50, (E) T3/T4 stage, (H) M0 stage, (I) M1 stage, (K) III/IV clinical stage and (M) G3/G4 grade.

3.6. SERPINB7 expression is associated with specific DEGs: identification and functional analyses

We investigated and annotated genes associated with SERPINB7 using the LinkedOmics database. The results are shown in Fig. 7A, where 339 genes (red dots) were found to be positively linked to SERPINB7, whereas 59 genes (blue dots) had negative associations. We selected 50 genes from the positively associated genes and 50 from the negatively associated genes and constructed the heatmap shown in Fig. 7B. The KEGG pathway and GO enrichment analyses assessed their potential involvement in specific molecular and

Table 2
Univariate and multivariate assessments for OS within CESC cases.

Characteristics	Univariate analysis			Multivariate analysis		
	Hazard ratio	95% CI	P value	Hazard ratio	95% CI	P value
Age	1.289	0.810–2.050	0.284			
T stage	3.863	2.072–7.201	**<0.001**	19.827	3.184–123.441	**0.001**
N stage	2.844	1.446–5.593	**0.002**	1.329	0.449–3.936	0.608
M stage	3.555	1.187–10.641	**0.023**	0.000	0.000-Inf	0.998
Clinical stage	2.369	1.457–3.854	**<0.001**	0.297	0.056–1.576	0.154
Histological type	1.033	0.543–1.969	0.920			
Histologic grade	0.866	0.514–1.459	0.589			
SERPINB7	1.194	1.038–1.372	**0.013**	1.674	1.140–2.457	**0.009**

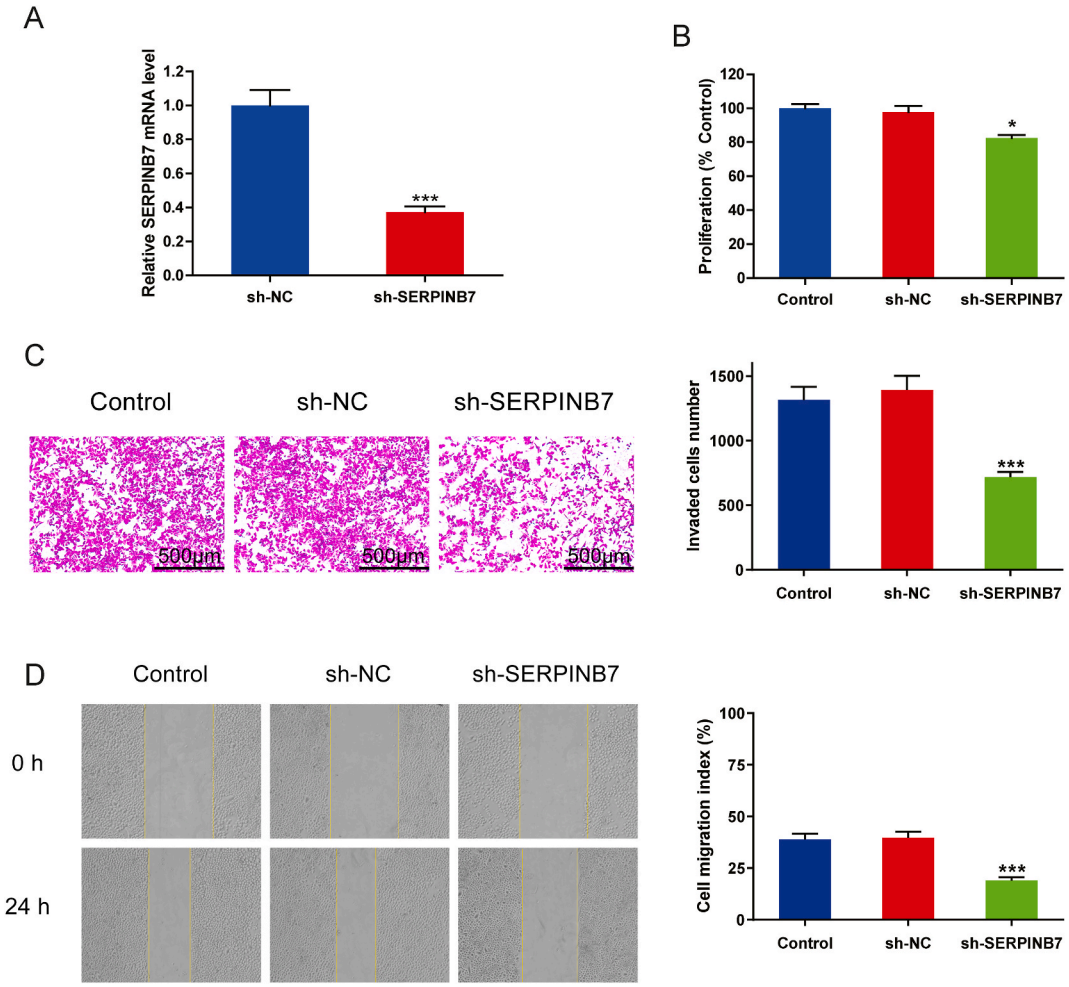

Fig. 5. Knockdown of SERPINB7 reduced CESC cell growth and invasion. (A) RT-qPCR detected the knockdown efficiency of sh-SERPINB7. (B) MTT cytotoxicity test showed that the growth ability of CESC cells decreased after SERPINB7 knockdown. (C) Transwell and (D) Scratch analysis showed that the invasion and migration abilities of CESC cells decreased after SERPINB7 knockdown. Error bars indicate the mean ± SD. *P < 0.05; ***P < 0.001.

biological processes. KEGG analysis indicated that the DEGs participated mainly in interleukin (IL)−17, cytokine−cytokine receptor interactions and estrogen signal transduction pathways. GO showed that the genes were significantly enriched in processes involving skin, epidermis, and keratinocyte growth and specialization (Fig. 7C).

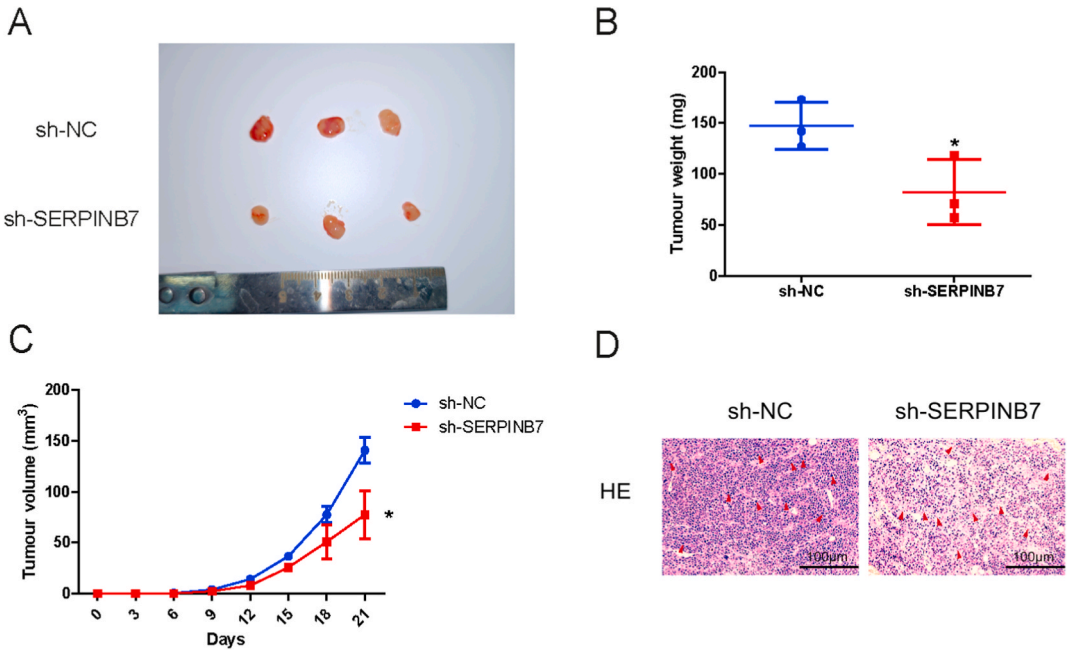

Fig. 6. Knockdown of SERPINB7 inhibited tumor development in CESC mouse models. Knockdown of SERPINB7 resulted in a decrease in (A) tumor size, (B) weight, (C) volume, and (D) histological grade (× 200). Error bars designate mean ± SD and * $P < 0.05$.

3.7. SERPINB7 expression is correlated with the TME

Associations between SERPINB7 expression and the TME in CESC were also examined. This showed a positive association between SERPINB7 expression and infiltration of neutrophils ($P < 0.001$), Tgds ($P < 0.001$), aDCs ($P = 0.033$), and Tcm cells ($P = 0.038$). Conversely, SERPINB7 was negatively associated with infiltration by NK cells ($P < 0.001$), pDCs ($P = 0.001$), Tems ($P = 0.003$), and TFHs ($P = 0.011$). These findings are illustrated in Fig. 8A–B. Furthermore, to understand the implications of SERPINB7 expression in the context of immunotherapy, we explored its prognostic values. The results revealed a negative relationship between SERPINB7 transcription levels and the expression of LAG3 and PDCD1, as shown in Fig. 8C. Together, these findings shed light on the potential functional roles of SERPINB7 and its interactions with specific genes in CESC, as well as its influence on the TME and implications for immunotherapy. The comprehensive understanding of these associations may contribute significantly to the development of targeted therapies and improved treatment strategies for cervical cancer.

3.8. SERPINB7 transcription levels in CESC and its response to chemotherapy

The previous sections provide valuable insights into the expression and associations of SERPINB7 in CESC, its correlation with the TME, and its prognostic implications for immunotherapy. Building upon this, section 3.8 explores the response of SERPINB7 transcription levels in CESC to chemotherapy, a standard therapeutic approach for advanced tumor stages. The chemotherapy drugs clinically used for CESC include Bleomycin, Cisplatin, Docetaxel, Gemcitabine, Methotrexate, Mitomycin C, and Paclitaxel. We investigated the IC_{50} values of these drugs to determine sensitivity to these chemotherapeutic agents. Our data demonstrated that cases where SERPINB7 was overexpressed had lower IC_{50} values for Bleomycin ($P = 6.5e{-}05$), Docetaxel ($P = 0.00075$), and Paclitaxel ($P = 9.8e{-}06$) but showed no differences for Cisplatin ($P = 0.091$), Gemcitabine ($P = 0.38$), Methotrexate ($P = 0.60$), and Mitomycin C ($P = 0.87$) (Fig. 9A–G).

3.9. SERPINB7 methylation is changed in CESC

Continuing from the previous section's exploration of the response of SERPINB7 transcription levels in CESC to chemotherapy, section 3.9 investigates the changes in SERPINB7 methylation in CESC. Through the analysis of SERPINB7 gene alterations in the two datasets, it was found that the proportion of these alterations was 1.01% (3/297) (Fig. 10A–B). Kaplan-Meier and log-rank tests revealed significant differences in both OS ($P = 4.178e{-}3$), DFS ($P = 0.0169$), and progression-free survival ($P = 4.07e{-}8$) between the altered and unaltered cohorts (Fig. 10C–E). Moreover, specific methylation CpG sites, including cg01568736, were found to have high DNA methylation (Fig. 10F), and one particular CpG methylation site, cg24349668, was associated with prognosis, where individuals with high SERPINB7 methylation of that CpG site exhibited superior OS (Table 3). These findings highlight the potential impact of SERPINB7 methylation on disease progression and patient outcomes in CESC, providing valuable insights into the epigenetic

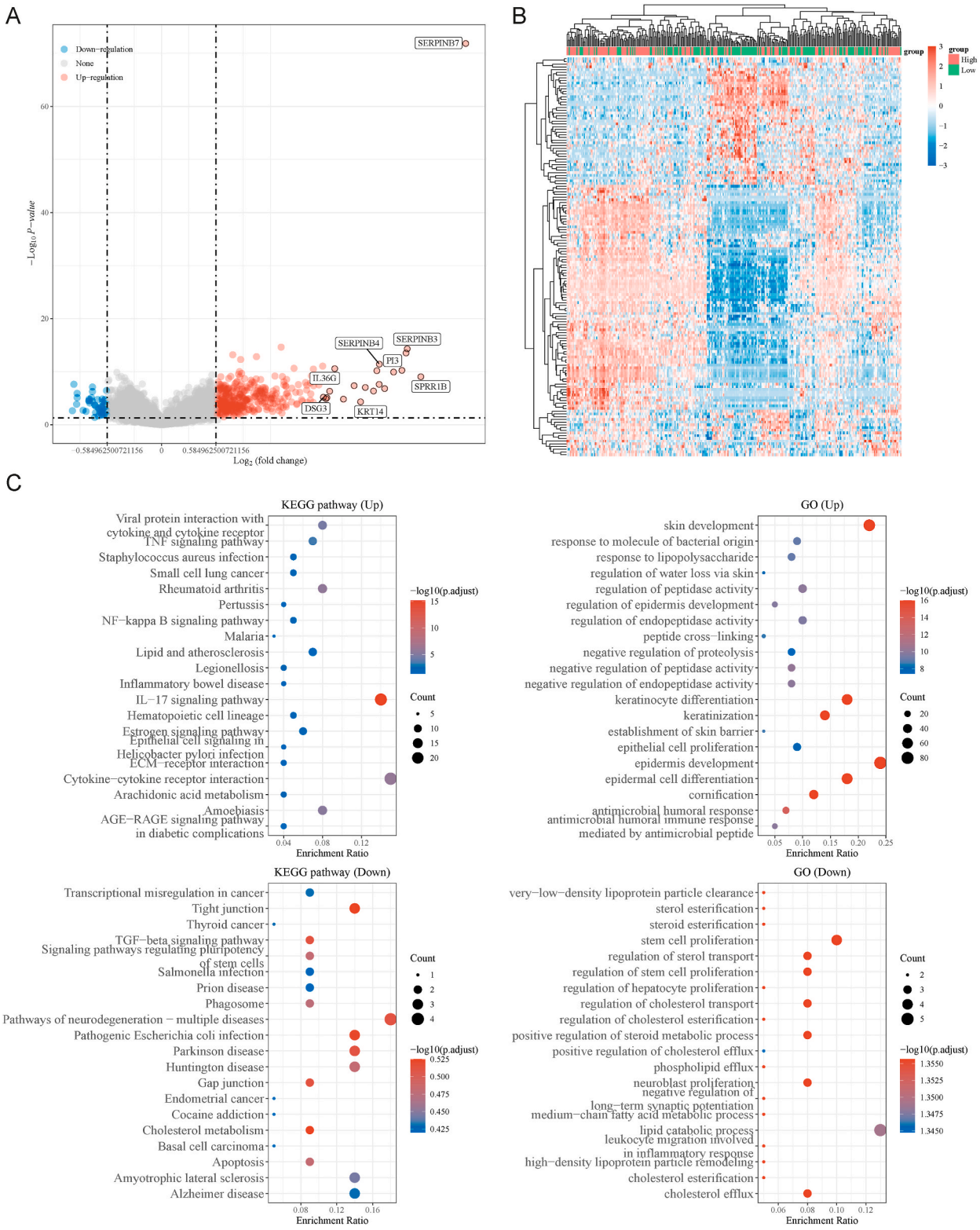

Fig. 7. Enrichment-based assessments for DEGs linked with SERPINB7. (A) Volcano plot and (B) heatmap showing DEGs associated with SERPINB7 expression Red/blue reflect up-/down-regulated genes respectively. (C) KEGG and GO assessments identified the specific molecular and biological processes in which the up-regulated and down-regulated DEGs may be involved.

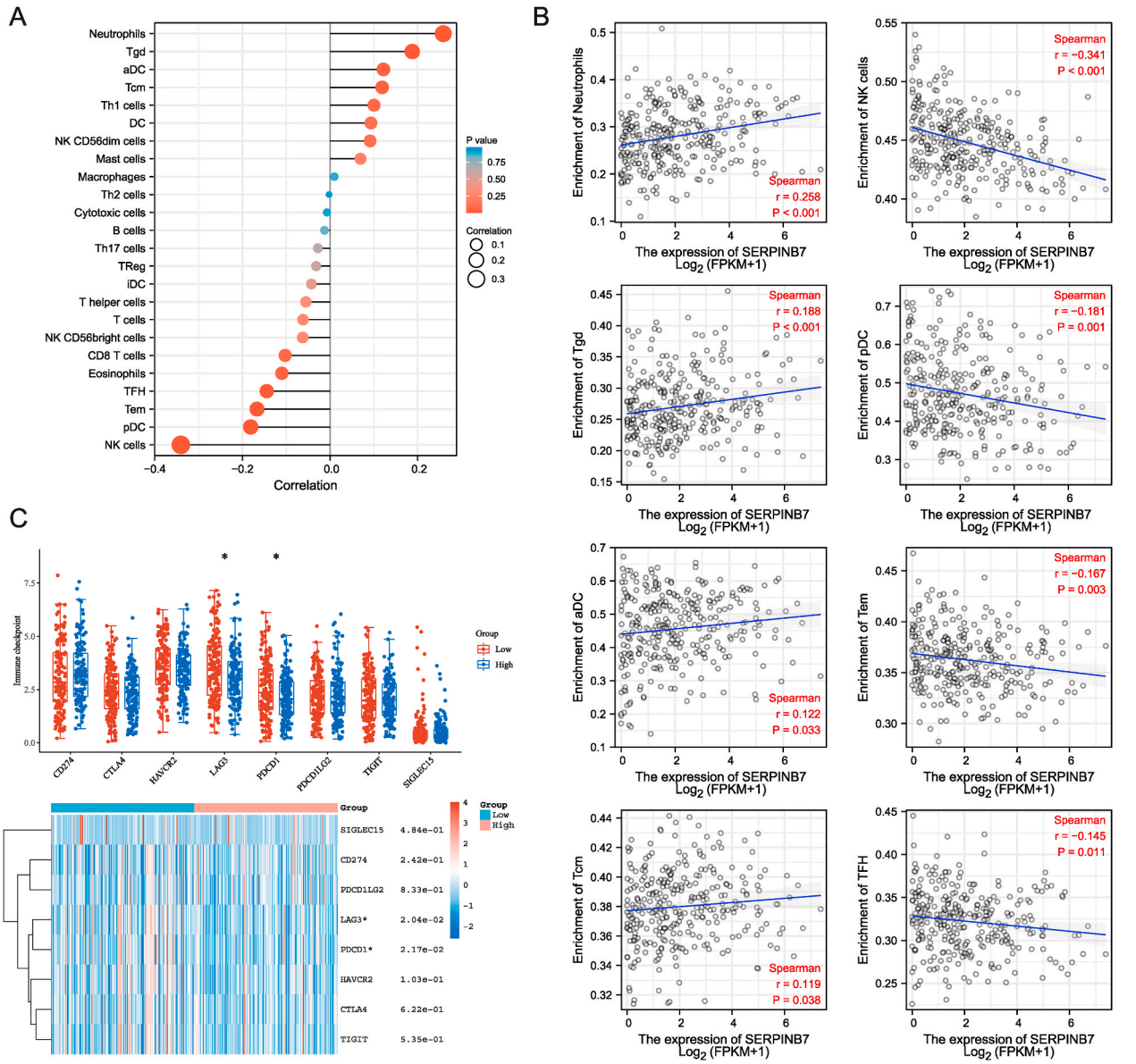

Fig. 8. TME immune cell infiltration analyses. (A) Forest plot and (B) Spearman correlation analysis revealed the correlation between infiltration levels of immune cells and SERPINB7 expression. (C) Comparative analyses for immune-checkpoint expression profiles across SERPINB7 low-/high-expressing cohorts. *P < 0.05.

regulation of this gene in the context of cervical cancer.

4. Discussion

As the primary symptoms of CESC are often undetectable, the disease progression may continue for 10 years. A neglect of routine physical examinations can lead to late diagnosis, thus missing the optimal period for treatment [17,18]. Consequently, the accuracy of the initial diagnosis is of major importance. CA125, CEA, and SCC are currently used clinical markers for CESC, but their accuracy is often poor. Therefore, the exploration of novel sensitive and specific serum CESC markers allowing the detection and early diagnosis of CESC is important, especially markers that may impact the TME in CESC.

Various studies have shown that the SERPINB family has a targeted biological activity function. It has been shown to be aberrantly expressed in many malignant cancers and significantly impacts tumor growth, cell death, and metastasis. Bianconi et al. found that SERPINB7 was expressed in primary and liver metastases of pancreatic cancer, with expression levels increasing with tumor progression. High expression of SERPINB7 mRNA was found to be associated with poor prognosis in pancreatic tumors [19]. Additionally,

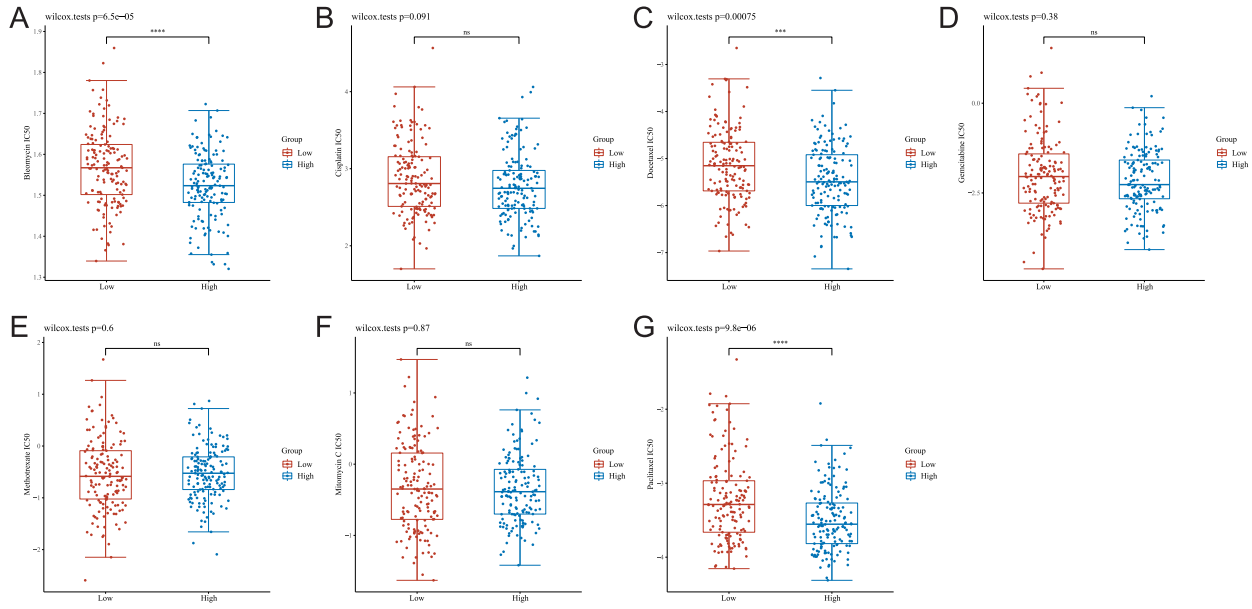

Fig. 9. Analysis of the correlation between SERPINB7 expression and sensitivity to chemotherapeutic drugs. Patients were categorized into high- and low-expression cohorts based on the median expression level of SERPINB7. Assessment of IC_{50} value for (A) Bleomycin, (B) Cisplatin, (C) Docetaxel, (D) Gemcitabine, (E) Methotrexate, (F) Mitomycin C and (G) Paclitaxel across SERPINB7 low-/high-expressing cohorts respectively. ns = not significant.

pancreatic tumor cells with high levels of SERPINB7 expression were associated with increased liver metastases, and the level of SERPINB7 in primary pancreatic cancer could be used as an indicator for predicting liver micrometastases after tumor resection [11]. Chou et al. showed that SERPINB7 was also overexpressed in lung and breast cancer tissues, but its overexpression inhibited tumor metastasis *in vitro* [12]. In addition, SERPINB7 was found to be downregulated in oral squamous cell carcinoma [20]. These findings indicate that both the levels and activities of SERPINB7 vary between different tumor types. However, there are currently insufficient studies on the role of SERPINB7 in tumors, and the specific mechanism is not well understood.

To the best of our knowledge, this is the first study to explore the correlation between SERPINB7 and the prognosis, immune microenvironment, and malignant behavior of CESC. This showed that SERPINB7 was significantly involved in tumor growth, the TME, and patient prognosis. Our data demonstrated that SERPINB7 was overexpressed in CESC compared with normal tissue samples. This was also confirmed in clinical samples. Further, we showed that SERPINB7 represents a promising biomarker for diagnosing CESC and was able to differentiate between early and late tumor stages, specifically stages I and IV. These results suggest the potential of using SERPINB7 expression as a biomarker in clinical practice. This is consistent with our results demonstrating that SERPINB7 upregulation correlated with poor prognosis, and the tumorigenic roles of SERPINB7 were confirmed in animal models, further verifying the hypothesis.

To clarify the mechanism underlying the involvement of SERPINB7 in CESC progression, we investigated DEGs linked to SERPINB7 expression. The GO analysis identified biological processes related to the development and differentiation of the epidermis and skin. Our results showed that these might be related to cancer biological processes, including cell differentiation and promotion of the epithelial-mesenchymal transition. KEGG analysis showed significant enrichment in IL-17-associated signal transduction. This pathway has been implicated in cancer caused by chronic inflammation where it was found to play a tumor-promoting role in the TME, activating precancerous cells to promote tumor proliferation and inhibiting anti-tumor immune responses [21–23]. These functions of IL-17 have been reported in many cancers, including cervical, breast, liver, and colorectal cancer, which are closely related to the incidence and progression of CESC [24–27].

In recent years, tumor immunity and metabolism in the TME have become the focus of anti-tumor therapy research. The TME includes both tumor cells and infiltrating immune cells such as T cells, B cells, macrophages, and NK cells [28]. The immune cells are involved in immune surveillance and anti-tumor activities. However, imbalances in immune regulation can lead to dysregulation, immune escape, and tumor development. This study found associations between SERPINB7 levels and the infiltration of neutrophils, Tgds, aDCs, Tcms, NK cells, pDCs, Tems, and TFHs.

Immune checkpoint inhibitors are expressed on the surfaces of immune cells, playing essential functions in keeping the immune system stable. Immunotherapy using monoclonal antibodies targeting immune checkpoints has made remarkable achievements in treating multiple advanced tumors [29]. We further found that patients with overexpression of SERPINB7 had downregulated expression of the classical immune checkpoint molecules LAG3 and PDCD1. The results indicated that cancer promotion by SERPINB7 relies on blocking the immune response. These results allowed us to speculate that elevated SERPINB7 levels would predict poorer cancer response to immunotherapy.

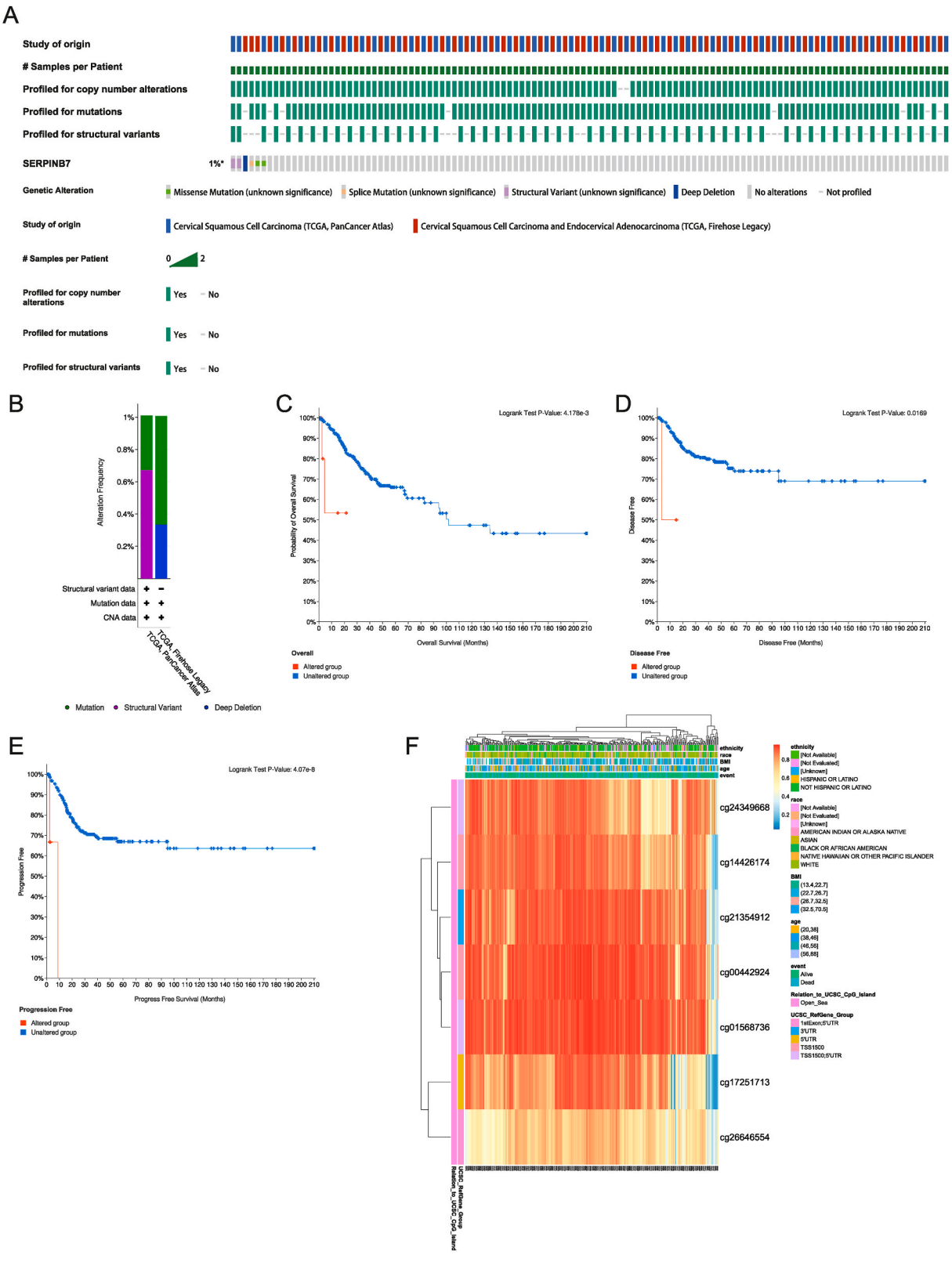

(caption on next page)

Fig. 10. Genetic alteration and methylation in SERPINB7 in CESC. (A) A visual summary of SERPINB7 alterations produced using OncoPrint. (B) Variations for SERPINB7 in CESC from TCGA, Firehose Legacy and TCGA, PanCancer Atlas databases. Kaplan-Meier curves analysis showed that patients with SERPINB7 gene alters resulted in unfavorable (C) OS, (D) DFS and (E) progression-free survival. (F) SERPINB7 methylation and expression levels were assessed.

Table 3
Effect of hypermethylation level on prognosis in CESC.

CpG	HR	P value
TSS1500-Open_Sea-cg00442924	1.273	0.3803
TSS1500; 5′UTR-Open_Sea-cg01568736	1.253	0.3859
TSS1500-Open_Sea-cg14426174	0.668	0.1878
5′UTR-Open_Sea-cg17251713	1.604	0.1127
3′UTR-Open_Sea-cg21354912	0.78	0.3928
TSS1500; 5′UTR-Open_Sea-cg24349668	0.581	**0.0255**
1stExon; 5′UTR-Open_Sea-cg26646554	0.811	0.3740

Gene mutations are strongly associated with cancer, typically with worse prognoses. We found that SERPINB7 in CESC had 1.01% mutations, significantly associated with poor OS. In recent years, with continuous advances in detection, the role of tumor epigenetics, especially changes in the DNA methylation of tumor biomarkers, has gained significant attention [30]. The development of clinical and medicinal strategies based on changes in DNA methylation has made major breakthroughs in tumor diagnosis, prognosis evaluation, and the prediction of treatment responses [31,32]. We further analyzed the underlying epigenetic mechanisms associated with tumor growth and highlighted the methylation of specific CpG islands that were predictive of CESC aggressiveness.

In recent years, progress in computational biology has yielded valuable insights into gene regulatory networks and molecular interactions relevant to various diseases by predicting molecular interactions. In the realm of tumor diseases like cervical cancer, the exploration of computational biology techniques in predicting interactions between genetic markers and non-coding RNAs has had promising results. Our forthcoming research will center on the use of computational models to predict non-coding RNA interactions [33–38], particularly focusing on miRNA-lncRNA interactions. This approach has the potential to uncover regulatory pathways that may significantly influence cervical cancer. Furthermore, it could provide deeper insights into their potential roles in the regulation of CESC growth, invasion, and metastasis.

The present study has several limitations. Firstly, most of the analyses were conducted *in silico,* utilizing data extracted from publicly available databases, resulting in a restricted number of patients being included in the investigation. This limitation poses challenges in substantiating the diagnostic and prognostic implications of the reported findings. Secondly, the study's scope lacked experimental verification of the upstream and downstream pathways associated with SERPINB7 which play a pivotal role in CESC. Such experimental verification is imperative for the comprehensive understanding of the molecular mechanisms underlying SERPINB7's role in CESC progression. Lastly, prospective studies are necessary to corroborate the predictive value of SERPINB7 in the context of CESC immunotherapy responses. Such rigorous prospective investigations are essential for translating the study's findings into potential clinical applications and therapeutic interventions.

5. Conclusion

We demonstrated that SERPINB7 expression levels represented predictive markers for CESC, especially in terms of immunotherapy. We believe that these findings will stimulate further research into the involvement of SERPINB7 in molecular pathways associated with CESC tumor progression and malignancy, thus offering a perspective for future targeted therapy.

Author contribution statement

Xian-Shuang Tong: Conceived and designed the experiments.
Rui-Feng Zhang: Performed the experiments; Wrote the paper.
Hua-Fang Wei; Yue-Chen Zhao: Analyzed and interpreted the data; Wrote the paper.

Ethics approval and informed consent

The study protocol was approved by the Medical Ethics Committee of the Second Hospital of Jilin University (NO.2022–107) and was conducted in accordance with the Declaration of Helsinki. Informed consent was obtained from all subjects for the acquisition of tissue specimens. Animal studies were conducted in compliance with ARRIVE guidelines for the reporting of animal experiments and were approved by the Animal Ethics Committee of Jilin University (NO. KT201902025).

Consent for publication

All authors have contributed to, read, and approved this submitted manuscript in its current form.

Data availability

All data generated or analyzed during this study are included in this published article. SERPINB7 transcription profiles of samples from CESC patients with their clinical and other relevant medical information were obtained from the TCGA platform (https://portal.gdc.cancer.gov/).

Funding

Not applicable.

Declaration of competing interest

The authors declare that they have no known competing financial interests or personal relationships that could have appeared to influence the work reported in this paper.

Acknowledgements

The technical guidance provided by the Department of Radiation Oncology at The Second Hospital of Jilin University in this study is greatly appreciated. The authors would like to thank all the reviewers who participated in the review and MJEditor (www.mjeditor.com) for its linguistic assistance during the preparation of this manuscript.

References

[1] M. Arbyn, E. Weiderpass, L. Bruni, et al., Estimates of incidence and mortality of cervical cancer in 2018: a worldwide analysis, Lancet Global Health 8 (2) (2020) e191–e203.
[2] T.A. Kessler, Cervical cancer: prevention and early detection, Semin. Oncol. Nurs. 33 (2) (2017) 172–183.
[3] S. Chopra, M. Gupta, A. Mathew, et al., Locally advanced cervical cancer: a study of 5-year outcomes, Indian J. Cancer 55 (1) (2018) 45–49.
[4] J.L. Sepulveda, Using R and bioconductor in clinical genomics and transcriptomics, J. Mol. Diagn. 22 (1) (2020) 3–20.
[5] B. Aslam, M. Basit, M.A. Nisar, M. Khurshid, M.H. Rasool, Proteomics: technologies and their applications, J. Chromatogr. Sci. 55 (2) (2017) 182–196.
[6] B.A. Merrick, R.E. London, P.R. Bushel, S.F. Grissom, R.S. Paules, Platforms for biomarker analysis using high-throughput approaches in genomics, transcriptomics, proteomics, metabolomics, and bioinformatics, IARC Sci. Publ. 163 (2011) 121–142.
[7] M. Gatto, L. Iaccarino, A. Ghirardello, et al., Serpins, immunity and autoimmunity: old molecules, new functions, Clin. Rev. Allergy Immunol. 45 (2) (2013) 267–280.
[8] A. Lucas, J.R. Yaron, L. Zhang, S. Ambadapadi, Overview of serpins and their roles in biological systems, Methods Mol. Biol. 1826 (2018) 1–7.
[9] A. Lucas, J.R. Yaron, L. Zhang, C. Macaulay, G. McFadden, Serpins: development for therapeutic applications, Methods Mol. Biol. 1826 (2018) 255–265.
[10] Z. Wang, H. Zheng, H. Zhou, et al., Systematic screening and identification of novel psoriasisspecific genes from the transcriptome of psoriasislike keratinocytes, Mol. Med. Rep. 19 (3) (2019) 1529–1542.
[11] A. Korekawa, E. Akasaka, D. Rokunohe, et al., Nagashima-type palmoplantar keratoderma and malignant melanoma in Japanese patients, Br. J. Dermatol. 180 (2) (2019) 415–416.
[12] R.H. Chou, H.C. Wen, W.G. Liang, et al., Suppression of the invasion and migration of cancer cells by SERPINB family genes and their derived peptides, Oncol. Rep. 27 (1) (2012) 238–245.
[13] G. Yu, L.G. Wang, Y. Han, Q.Y. He, clusterProfiler: an R package for comparing biological themes among gene clusters, OMICS 16 (5) (2012) 284–287.
[14] R. Ravi, K.A. Noonan, V. Pham, et al., Bifunctional immune checkpoint-targeted antibody-ligand traps that simultaneously disable TGFbeta enhance the efficacy of cancer immunotherapy, Nat. Commun. 9 (1) (2018) 741.
[15] D. Zeng, M. Li, R. Zhou, et al., Tumor microenvironment characterization in gastric cancer identifies prognostic and immunotherapeutically relevant gene signatures, Cancer Immunol. Res. 7 (5) (2019) 737–750.
[16] Q. Jiang, J. Sun, H. Chen, et al., Establishment of an immune cell infiltration score to help predict the prognosis and chemotherapy responsiveness of gastric cancer patients, Front. Oncol. 11 (2021), 650673.
[17] A. Derbie, B. Amare, E. Misgan, et al., Histopathological profile of cervical punch biopsies and risk factors associated with high-grade cervical precancerous lesions and cancer in northwest Ethiopia, PLoS One 17 (9) (2022), e0274466.
[18] L.L. Ring, C. Munk, M. Galanakis, J.E. Tota, L.T. Thomsen, S.K. Kjaer, Incidence of cervical precancerous lesions and cervical cancer in Denmark from 2000 to 2019: population impact of multi-cohort vaccination against human papillomavirus infection, Int. J. Cancer 152 (7) (2023) 1320–1327.
[19] D. Bianconi, G. Heller, D. Spies, et al., Biochemical and genetic predictors of overall survival in patients with metastatic pancreatic cancer treated with capecitabine and nab-paclitaxel, Sci. Rep. 7 (1) (2017) 4851.
[20] M. Shiiba, H. Nomura, K. Shinozuka, et al., Down-regulated expression of SERPIN genes located on chromosome 18q21 in oral squamous cell carcinomas, Oncol. Rep. 24 (1) (2010) 241–249.
[21] S.H. Chang, T helper 17 (Th17) cells and interleukin-17 (IL-17) in cancer, Arch Pharm. Res. (Seoul) 42 (7) (2019) 549–559.
[22] X. Li, R. Bechara, J. Zhao, M.J. McGeachy, S.L. Gaffen, IL-17 receptor-based signaling and implications for disease, Nat. Immunol. 20 (12) (2019) 1594–1602.
[23] M.J. McGeachy, D.J. Cua, S.L. Gaffen, The IL-17 family of cytokines in health and disease, Immunity 50 (4) (2019) 892–906.
[24] Y. Bai, H. Li, R. Lv, Interleukin-17 activates JAK2/STAT3, PI3K/Akt and nuclear factor-kappaB signaling pathway to promote the tumorigenesis of cervical cancer, Exp. Ther. Med. 22 (5) (2021) 1291.
[25] S. Razi, B. Baradaran Noveiry, M. Keshavarz-Fathi, N. Rezaei, IL-17 and colorectal cancer: from carcinogenesis to treatment, Cytokine 116 (2019) 7–12.
[26] X. Song, C. Wei, X. Li, The potential role and status of IL-17 family cytokines in breast cancer, Int. Immunopharm. 95 (2021), 107544.
[27] M. Zang, Y. Li, H. He, et al., IL-23 production of liver inflammatory macrophages to damaged hepatocytes promotes hepatocellular carcinoma development after chronic hepatitis B virus infection, Biochim. Biophys. Acta, Mol. Basis Dis. 1864 (12) (2018) 3759–3770.
[28] G.L. Beatty, W.L. Gladney, Immune escape mechanisms as a guide for cancer immunotherapy, Clin. Cancer Res. 21 (4) (2015) 687–692.
[29] S. Bagchi, R. Yuan, E.G. Engleman, Immune checkpoint inhibitors for the treatment of cancer: clinical impact and mechanisms of response and resistance, Annu. Rev. Pathol. 16 (2021) 223–249.
[30] Y. Pan, G. Liu, F. Zhou, B. Su, Y. Li, DNA methylation profiles in cancer diagnosis and therapeutics, Clin. Exp. Med. 18 (1) (2018) 1–14.
[31] V. Constancio, S.P. Nunes, R. Henrique, C. Jeronimo, DNA methylation-based testing in liquid biopsies as detection and prognostic biomarkers for the four major cancer types, Cells 9 (3) (2020).
[32] C.E. Lau, O. Robinson, DNA methylation age as a biomarker for cancer, Int. J. Cancer 148 (11) (2021) 2652–2663.

[33] L. Zhang, P. Yang, H. Feng, Q. Zhao, H. Liu, Using network distance analysis to predict lncRNA-miRNA interactions, Interdiscip Sci 13 (3) (2021) 535–545.
[34] F. Sun, J. Sun, Q. Zhao, A deep learning method for predicting metabolite-disease associations via graph neural network, Briefings Bioinf. 23 (4) (2022).
[35] W. Wang, L. Zhang, J. Sun, Q. Zhao, J. Shuai, Predicting the potential human lncRNA-miRNA interactions based on graph convolution network with conditional random field, Briefings Bioinf. 23 (6) (2022).
[36] H. Gao, J. Sun, Y. Wang, et al., Predicting metabolite-disease associations based on auto-encoder and non-negative matrix factorization, Briefings Bioinf. (2023).
[37] H. Hu, Z. Feng, H. Lin, et al., Gene function and cell surface protein association analysis based on single-cell multiomics data, Comput. Biol. Med. 157 (2023), 106733.
[38] T. Wang, J. Sun, Q. Zhao, Investigating cardiotoxicity related with hERG channel blockers using molecular fingerprints and graph attention mechanism, Comput. Biol. Med. 153 (2023), 106464.